Science of the Total Environment 833 (2022) 155187

Contents lists available at ScienceDirect

Science of the Total Environment

journal homepage: www.elsevier.com/locate/scitotenv

Rethinking the biotic and abiotic remineralization of complex phosphate molecules in soils and sediments

Biao Wan [a], Rixiang Huang [b], Julia M. Diaz [c], Yuanzhi Tang [a,*]

[a] School of Earth and Atmospheric Sciences, Georgia Institute of Technology, Atlanta, GA 30332-0340, USA
[b] Department of Environmental and Sustainable Engineering, University at Albany, State University of New York, 1400 Washington Ave, Albany, NY 12222-0100, USA
[c] Geosciences Research Division, Scripps Institution of Oceanography, University of California San Diego, La Jolla, CA 92093-5004, USA

HIGHLIGHTS

- The remineralization rates of complex P molecules by phosphatases and minerals are compared.
- The overlooked role of natural minerals as abiotic catalyst for P remineralization is quantitatively evaluated.
- Enzymes and oxide minerals have different preferences for organic P and phosphoanhydride hydrolysis.
- The normalized rates of abiotic and biotic P hydrolysis are comparable for phosphoanhydrides.
- Natural minerals can be abiotic catalysts for P remineralization in addition to being an absorbent for P sequestration.

GRAPHICAL ABSTRACT

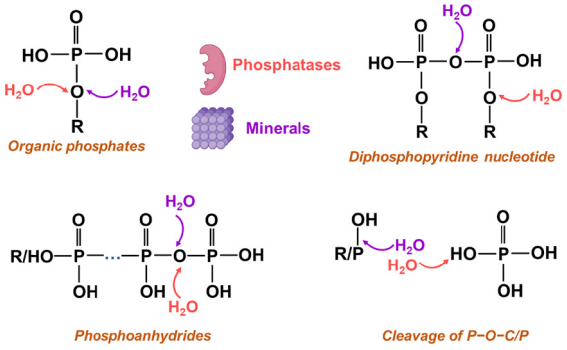

ARTICLE INFO

Editor: Daniel Alessi

Keywords:
Remineralization
Phosphatases
Minerals
Organic phosphates
Phosphoanhydrides

ABSTRACT

Phosphorus (P) is an essential macronutrient for all living organisms. Despite a diversity of P compounds in the environment, orthophosphate is the most bioavailable form of P. Remineralization of complex P molecules (e.g., organic P and phosphoanhydrides) into orthophosphate is traditionally considered to be carried out primarily by enzymes. Natural minerals are recently viewed to be abiotic catalysts (as compared to the organic phosphatases) to facilitate the cleavage of terminal P–O–C/P bonds and remineralization of complex P compounds. However, quantitative comparison between biotic and abiotic remineralization pathways of complex P molecules is still missing, impeding our capability to assess the importance and contribution of abiotic P remineralization in the environment. This study compares the hydrolysis rates of six organic phosphates and three inorganic phosphoanhydrides by representative enzymes (acid and alkaline phosphatases) and natural oxide minerals (hematite, birnessite, and boehmite). The results show that enzymes and minerals have different substrate preferences. Specifically, alkaline phosphatase hydrolyzes phosphate monoesters faster than phosphoanhydrides, whereas acid phosphatase and minerals show higher hydrolysis rates toward phosphoanhydrides than phosphate monoesters. Although the hydrolysis rates by enzymes (~μM hr^{-1}) are orders of magnitude higher than those by minerals (~μM d^{-1}), normalization of the rates by the natural abundance of enzymes and minerals leads to comparable contributions of both processes in soils and sediments. These results highlight the significance of natural minerals in the remineralization of complex P compounds, a process that was traditionally overlooked but with important implications for constraining P biogeochemical cycling in the environment.

* Corresponding author.
E-mail address: yuanzhi.tang@eas.gatech.edu (Y. Tang).

http://dx.doi.org/10.1016/j.scitotenv.2022.155187
Received 20 December 2021; Received in revised form 5 April 2022; Accepted 7 April 2022
Available online 11 April 2022

1. Introduction

Phosphorus (P) is an essential element for all life as the building block of many structural and functional components of organisms (Karl, 2014; Paytan and McLaughlin, 2007). As one of the most abundant elements on Earth, P has an average crustal abundance of 0.1% by weight (Canfield et al., 2005). Total P concentration is estimated to be 170–21,000 mg kg^{-1} in surface and subsurface environments (e.g., soils and sediments) (Klein et al., 2019). However, P is always viewed as a potentially limiting macronutrient for terrestrial and marine primary production (Ruttenberg, 2014; Thingstad et al., 2005).

Different P-containing compounds occur in nature, including orthophosphate, organic P esters, phosphoanhydrides, phosphite, and phosphonates, etc. (Figueroa and Coates, 2017; Paytan and McLaughlin, 2007; Van Mooy et al., 2015). Orthophosphate is typically considered as the most common P compound in surface environments and the only P form that can be directly and effectively taken up by most of living organisms, although recent studies showed that some microorganisms can utilize low weight dissolved organic phosphates and reduced forms of P (Karl, 2014; Van Mooy et al., 2015). Once external P inputs are limited, local P recycling is of great importance for P supply and organism survival (Chen et al., 2018; Zhu et al., 2018) since a large fraction of total P pool consists of organic phosphates (9.3–69.2%) and inorganic phosphoanhydrides (0.4–13.0%) (Diaz et al., 2008; Liu et al., 2018; Recena et al., 2018; Wan et al., 2019b). For example, in open oceans, ~ 90% of gross primary production is supported by local hydrolysis and recycling of organic phosphates and phosphoanhydrides, mainly driven by microbial P assimilation and remineralization (Karl, 2014). The remineralization of organic phosphates into orthophosphate by microorganisms can alleviate P starvation, and phosphatases are typically synthesized in response to phosphate depletion, assisting with P acquisition (Duhamel et al., 2021; Lidbury et al., 2022). The hydrolysis and recycling of organic phosphates (e.g., phosphate monoesters) and phosphoanhydrides (e.g., pyrophosphate and polyphosphate) could thus significantly influence global biogeochemical processes and globe primary productivity via the alleviation of P starvation and the assistance with P acquisition (Baldwin, 2013; Ruttenberg, 2014; Van Mooy et al., 2015).

In natural environments, the movement of P among different reservoirs is generally regulated by biotic (e.g., remineralization, uptake, release, and assimilation) and abiotic processes (e.g., adsorption, desorption, dissolution, and precipitation) (Defforey and Paytan, 2018; Ruttenberg, 2014). Due to the high specificity and high reaction rates, enzymatic hydrolysis of phosphate esters and phosphoanhydrides – a biotic process – is traditionally viewed as the main mechanism for the degradation of complex P molecules to produce bioavailable orthophosphate (Huang et al., 2018; Olsson et al., 2012). Typical extracellular enzymes such as acid and alkaline phosphatases can rapidly catalyze the breakage of phosphate ester (P – O – C) and terminal phosphoanhydride (P – O – P) bonds, leading to the hydrolysis of organic phosphates and polyphosphates to produce orthophosphate (Huang et al., 2018; Jarosch et al., 2019).

Meanwhile, natural oxide minerals are always considered as an important abiotic factor in P sequestration and regulating global P cycling, though their specific roles still need to be better constrained (Klein et al., 2019; Wan et al., 2019b; Wood et al., 1984). Iron (Fe) and aluminum (Al) oxide minerals have large surface areas and highly positive surface charges under typical environmental conditions, and are able to uptake large amounts of phosphate via surface adsorption, incorporation, and/or precipitation. Thus, these minerals are traditionally viewed as a sink or source of P in aquatic and soil environments (Ruttenberg and Sulak, 2011; Wang et al., 2016; Yan et al., 2014). Manganese (Mn) oxides, another common group of metal oxide mineral in natural environments, are negatively charged at circumneutral pH conditions and thus generally have a low affinity for phosphate adsorption.

In addition to the roles of Fe, Al, and Mn oxides as absorbents for P sequestration, a few recent studies showed that these minerals can act as abiotic catalysts and enable the rapid hydrolysis/remineralization of phosphate esters and phosphoanhydrides into orthophosphate via the cleavage of P—O—C or P – O–P bonds, a process that shares similar mechanism as enzymatic P hydrolysis (Huang, 2018; Klein et al., 2019; Wan et al., 2019a; Wan et al., 2021). The rate of Mn oxide-catalyzed hydrolysis of organic phosphate ester is reported to be an order of magnitude higher than Fe and Al oxides (Baldwin et al., 1995). These studies provided a new angle to evaluate the potentially critical yet overlooked roles of natural minerals in P remineralization and recycle. Despite the previous studies on phosphatase- and mineral-catalyzed hydrolysis of organic phosphate esters and phosphoanhydrides (Huang et al., 2018; Huang, 2018; Wan et al., 2019b), direct quantification and comparison of P remineralization rates via biotic (enzyme) and abiotic (mineral) pathways are still missing (Duhamel et al., 2021).

In this study, we hypothesize that, in addition to the traditional view of being a P *sink* or *source*, natural oxide minerals can assist P hydrolysis and acquisition by serving as abiotic *catalysts* to facilitate the degradation of complex P molecules. We systematically compare and evaluate the hydrolysis of nine representative P compounds in the presence of two common P enzymes (acid and alkaline phosphatases) and the most common phases of Fe, Al, and Mn oxide minerals (hematite, boehmite, and birnessite). To our knowledge, the results provide the first quantitative comparison of biotic (enzyme) and abiotic (mineral) hydrolysis rates of these nine common phosphate compounds. ^{31}P nuclear magnetic resonance (NMR) spectroscopy was conducted to determine the preferential hydrolysis of organic phosphate monoester and polyphosphate by enzymes and minerals. By estimating the environmental distribution and abundance of these phosphates and oxide minerals in soils and sediments, we provide an initial assessment of the relative contributions of these biotic and abiotic pathways in governing P transformation and remineralization in soils and sediments.

2. Materials and methods

2.1. Materials and reagents

Nine selected P-containing compounds (details in Table 1) were obtained from MilliporeSigma, including six organic phosphates: β-glycerophosphate (GP), D-glucose 6-phosphate (G6P), adenosine 5′-monophosphate (AMP), adenosine 5′-triphosphate (ATP), diphosphopyridine nucleotide (NP), and *myo*-inositol hexakisphosphate (IHP), as well as three inorganic phosphoanhydrides: pyrophosphate (P_2), tripolyphosphate (P_3), and polyphosphate (with 45 P unit, P_{45}). Beside phosphate monoester P—O—C bond, ATP and NP also contain phosphoanhydride P—O—P bond (Table 1). These nine P compounds represent the most abundant organic phosphates and phosphoanhydrides in the environment. Enzyme and mineral-catalyzed hydrolysis experiments were conducted using two common enzymes (acid and alkaline phosphatases, both from MilliporeSigma) and three most common Fe, Mn, and Al oxide minerals (hematite, birnessite, and boehmite, respectively). Information on the source, synthesis, and characterization of all materials are in Supplementary Materials (SM) *Text S1* and Table 1.

2.2. Hydrolysis experiments

The two enzymatic experiments were conducted at different pH values (acid phosphatase at pH 6 and alkaline phosphatase at pH 8) for optimal enzymatic activity as suggested by the manufacturer. The optimal pH range is 4–7 for acid phosphatase (Hoehamer et al., 2005) and 6–11 for alkaline phosphatase (Golotin et al., 2015; Hoehamer et al., 2005). Our selected pH conditions of 6 and 8 are representative of environment conditions such as freshwater and seawater. For enzymatic hydrolysis of P compounds, phosphatase stock solutions were prepared at 2 units mL^{-1} in a 0.01 M 3-(N-morpholino)-propanesulfonic acid (MOPS) buffer at pH 6 (for acid phosphatase) or a 0.01 M 4-(2-hydroxyethyl)-1-piperazineethanesulfonic acid (HEPES) buffer at pH 8 (for alkaline phosphatase). In 15 mL centrifuge tubes, 8.3 mL deionized (DI) water containing 0.01 M MOPS buffer or

Table 1
Label, type, chemical formula, structure, and stock solution concentrations of the organic phosphate and phosphoanhydride compounds used in this study.

Label	Type	Compounds and chemical formula	Structure[a]	Concentration of stock solution [b]
GP	Phosphomonoester	β-Glycerophosphate disodium salt hydrate $(HOCH_2)_2CHOP(O)(ONa)_2{\cdot}xH_2O$	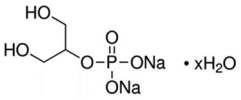	50 mM in total P (0.047 ± 0.001%)
G6P	Phosphomonoester	D-Glucose 6-phosphate disodium salt hydrate $C_6H_{11}Na_2O_9P{\cdot}xH_2O$	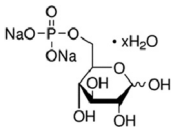	50 mM in total P (0.717 ± 0.003%)
NP	Phosphomonoester/Phosphoanhydride	Diphosphopyridine nucleotide $C_{21}H_{27}N_7O_{14}P_2{\cdot}xH_2O$	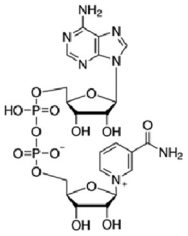	40 mM in total P (0.027 ± 0.005%)
AMP	Phosphomonoester	Adenosine 5′-monophosphate monohydrate $C_{10}H_{14}N_5O_7P{\cdot}H_2O$	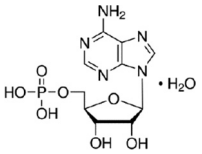	50 mM in total P (0.044 ± 0.002%)
ATP	Phosphomonoester/Phosphoanhydride	Adenosine 5′-triphosphate disodium salt hydrate $C_{10}H_{14}N_5Na_2O_{13}P_3{\cdot}xH_2O$	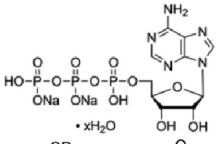	20 mM in total P (1.245 ± 0.026%)
IHP	Phosphomonoester	Phytic acid sodium salt hydrate $C_6H_6O_{24}P_6{\cdot}12Na$	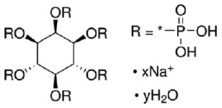	60 mM in total P (3.325 ± 0.041%) [c]
P_2	Phosphoanhydride	Sodium pyrophosphate decahydrate $Na_4P_2O_7$	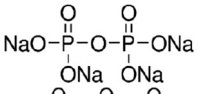	40 mM in total P (0.394 ± 0.133%)
P_3	Phosphoanhydride	Sodium tripolyphosphate $Na_5P_3O_{10}$	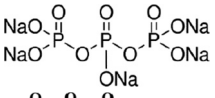	20 mM in total P (0.629 ± 0.057%)
P_{45}	Phosphoanhydride	Sodium phosphate glass, type 45	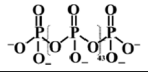	40 mg L^{-1} (~45 mM) in total P (0.528 ± 0.051%)

[a] Structures of GP, G6P, NP, AMP, ATP, IHP, P_2 and P_3 are from manufacturer (MilliporeSigma).
[b] Percent values in the parentheses indicate the amount of hydrolyzed P in the stock solution after 120-day storage.
[c] 3.325% hydrolysis attributes to pre-existed orthophosphate in IHP salts with 97% purity.

0.01 M HEPES buffer was mixed with calculated volumes of phosphate stock solution (~0.2 mL; details in Table 1), 0.5 mL of 2 M NaCl solution, and 1 mL phosphatase stock solution to achieve a total P concentration of ~1 mM and enzyme concentration of 200 units L^{-1}. The use of MOPS/HEPES buffers maintained the solution pH within ±0.1 unit.

To explore the effects of divalent metal cations (Ca^{2+}, Mg^{2+}, Zn^{2+}, and Mn^{2+}) on the enzymatic hydrolysis, parallel experiments were conducted by adding 0.1 mL of 50 mM metal stock solution to the centrifuge tubes to achieve a metal concentration of 0.5 mM. All experiments were performed in a shaking incubator at 225 rpm and 37 °C. At different time points, 50 μL aliquot of solution was sampled and immediately analyzed for orthophosphate production using the phosphomolybdate colorimetric assay (Murphy and Riley, 1962) on an UV–vis spectrometer (Carey 60, Agilent). We note that the observed orthophosphate production is slightly higher than 1000 μM for P_{45} hydrolysis by acid phosphatase, likely because the chemical formula of P_{45} is unknown, thus making it difficult to accurately calculate P_{45} concentration as total P. However, it does not affect the reaction trends and conclusions.

For mineral-catalyzed hydrolysis experiments, 500 mL of 2.4 g L^{-1} hematite, birnessite, and boehmite stock suspensions were prepared at deserved pH and equilibrated overnight under magnetic stirring. Then, 22.45 mL DI water containing 0.01 M MOPS or HEPES buffer was mixed with P stock solution (~ 0.75 mL), 0.3 mL of 50 mM Ca^{2+} stock solution, 1.5 mL of 2 M NaCl stock solution, and 5.0 mL of 2.4 g L^{-1} mineral stock suspension in a 50 mL glass bottle to achieve a total P concentration of ~1 mM and mineral concentration of 0.4 g L^{-1}. pH value of the reaction suspension was monitored and adjusted using 0.1 M HCl or NaOH if needed. To explore the effects of metal cations (Mg^{2+}, Zn^{2+}, and Mn^{2+}, and a control with no metal addition), parallel experiments were conducted by adding 0.3 mL of 50 mM metal stock solutions to the 50 mL glass bottles to achieve a metal concentration of 0.5 mM. Varied amount of DI water was added to achieve the same total volume of reaction suspension. All reaction suspensions were constantly agitated. At specific time points, 0.5 mL suspension was taken, immediately centrifuged, and filtered through a 0.22-μm Millipore membrane, and 50 μL of the supernatant was used to analyze orthophosphate concentration. To prevent microbial growth, 10 μL of

5 mM sodium azide (NaN_3) solution was added to the reaction suspensions at selected time points. The stability of the nine phosphates stock solutions (without enzyme or mineral) was monitored over 120-day storage. The results (Table 1) show that spontaneous hydrolysis of these phosphates was limited. These experiments were considered as no-enzyme/mineral controls. All experiments were performed in at least duplicates.

2.3. Solution ^{31}P NMR analysis

To compare the preferential hydrolysis of organic phosphates and phosphoanhydrides by phosphatases and oxide minerals, the hydrolysis kinetics of GP and P_{45} were monitored using time-resolved ^{31}P solution NMR spectroscopy. GP and P_{45} were chosen as representative organic phosphate monoester and polyphosphate in natural environments.

For enzymatic hydrolysis of co-present GP and P_{45}, 498.5 μL DI water containing 0.01 M MOPS (pH 6, for acid phosphatase) or 0.01 M HEPES buffer (pH 8, for alkaline phosphatase) was mixed with 17.5 μL P_{45} stock solution, 14 μL GP stock solution, 100 μL deuterium oxide (D_2O), and 70 μL phosphatase stock solution in the NMR sample tubes to achieve a total P concentration of ~2 mM with ~1 mM P_{45} (as total P) and ~1 mM GP. In order to collect good NMR spectra with acceptable signal-to-noise ratio, total P concentration with GP and P_{45} were set up to 2 mM (Wan et al., 2019b). The use of 1 mM total P concentration for P_{45} is equivalent to 22.2 μM P_{45} molecules, much lower than GP. Thus, the absolute rates of hydrolysis between these two substrates for the same enzyme or mineral might not be directly comparable; in these experiments, we primarily focus on the relative *trends* of orthophosphate production and P_{45}/GP degradation. NMR spectra were collected immediately after the addition of phosphatase stock solution and at varied time points (0, 0.5, 1.5, 4, 8.5, 24, and 48 h) at room temperature (22 °C).

For mineral-catalyzed hydrolysis of co-present GP and P_{45}, 12.9 mL DI water containing 0.01 M MOPS or HEPES buffer was mixed with 0.5 mL P_{45} stock solution, 0.4 mL GP stock solution, 0.2 mL of 50 mM Ca^{2+} stock solution, 1 mL of 2 M NaCl stock solution, and 5.0 mL of 1.6 g L^{-1} mineral stock suspension in a 50 mL glass bottle. The final mineral concentration is 0.4 g L^{-1} and total P concentration is ~2 mM with ~1 mM P_{45} (as total P) and ~1 mM GP. At specific time points (4 h and 1, 3, 5, 7, 8, 9, 14, 18, and 24 d), 1.5 mL suspension was taken, immediately centrifuged, and filtered through a 0.22-μm Millipore membrane, and 0.8 mL supernatant and 0.2 mL D_2O was finally mixed to perform solution ^{31}P NMR spectroscopy. pH values of the reaction suspensions were monitored and adjusted to be target pH if needed before the sampling.

Solution ^{31}P NMR spectra were collected on a Bruker AMX 400 MHz spectrometer operated at 162 MHz and 297 K. Parameters of 90° pulse width, 6.5 k data points (TD) over an acquisition time of 0.51 s, and relaxation delay of 15 s were applied. Chemical shift was calibrated using 85% H_3PO_4 as the external standard. At least 256 scans (~0.5 h) were collected for each sample.

3. Results and discussion

3.1. Overall hydrolysis trends

The production of orthophosphate was applied to evaluate the hydrolysis rates in this study. Due to the large matrix of P compounds, enzymes, and minerals studied, we first compare the representative kinetic curves of polyphosphate (P_{45}) hydrolysis by acid and alkaline phosphatases, hematite, boehmite, and birnessite (Fig. 1). Acid phosphatase shows a higher rate for P_{45} hydrolysis than alkaline phosphatase, and both enzymes show much higher rates than hematite, boehmite, and birnessite. For the three minerals, hematite shows a higher rate and extent for P_{45} hydrolysis at pH 8 after 17 or 24 days, followed by birnessite and boehmite.

We then compare the hydrolysis of six organic phosphates (GP, G6P, NP, AMP, ATP, and IHP) and three inorganic phosphoanhydrides (P_2, P_3, and P_{45}) by phosphatases and minerals (Fig. 2) at pH 6 and 8. Acid and alkaline phosphatases can rapidly hydrolyze organic phosphate monoesters

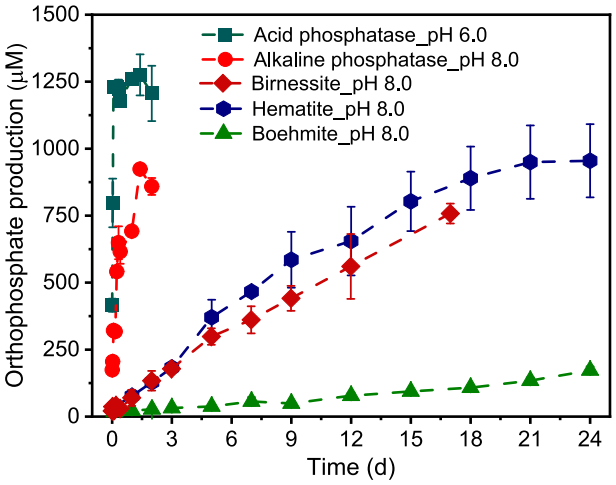

Fig. 1. Hydrolysis of polyphosphate (P_{45}) by phosphatases and minerals. Acid and alkaline phosphatases are the most common enzymes for P hydrolysis in natural environments. Hematite, birnessite, and boehmite represent common Fe, Mn, and Al (oxyhydr)oxide minerals in soils and sediments. Enzymatic experiments were conducted at different pH values (acid phosphatase at pH 6 and alkaline phosphatase at pH 8) for optimal enzymatic activity as suggested by the manufacturer, which are representative of environment pH conditions. Error bars indicate standard deviation (SD) of replicate experiments.

and inorganic phosphoanhydrides, except for IHP (a phosphate monoester) (Fig. 2a-f). Due to the steric structure, IHP resists rapid hydrolysis and a previous study indicated that IHP hydrolysis was limited to enzymatic reactions (Jarosch et al., 2019). Acid phosphatase can slowly hydrolyze NP (containing both phosphate ester and phosphoanhydride bonds), whereas orthophosphate production is limited through the hydrolysis by alkaline phosphatase (Fig. 2a and d). The limited production of orthophosphate from NP reaction with alkaline phosphatase suggests the low ability of alkaline phosphatase to cleave phosphoanhydride bonds within NP. For the three mineral systems, all phosphate compounds are slowly hydrolyzed, and after 17 or 24 days the hydrolysis extents of phosphoanhydrides (ATP, P_2, P_3 and P_{45}) are much higher than those of phosphate monoesters (GP, G6P, AMP, and IHP) and NP (Fig. 2g-o). For example, the hydrolysis extents of inorganic phosphoanhydrides and organic phosphates by three oxide minerals are in the range of 11.5–93.1% and 1.5–30.1%, respectively.

3.2. Kinetic fitting of hydrolysis rates

To provide an initial quantitative comparison of the hydrolysis rates of different experiments, we performed kinetic fitting for orthophosphate production during enzyme- and mineral-catalyzed hydrolysis of phosphate esters and phosphoanhydrides. In previous studies, mineral-catalyzed hydrolysis curves were fitted as first order kinetic reactions (Huang et al., 2018; Wan et al., 2019b) and enzymatic hydrolysis was fitted using the Michaelis–Menten equation (Jarosch et al., 2019). In order to obtain an initial direct comparison between the enzyme and mineral systems, here we first use linear fitting of the rates during the initial reaction stages. The fitted hydrolysis rates are summarized in Fig. 3 and the fitting curves are presented in Fig. S1. The linear fitting parameters (Table S1) show that NP and IHP have very low hydrolysis rates (a few μM hr^{-1}) by both acid and alkaline phosphatases, as compared to the higher rates (hundreds of μM hr^{-1}) of other seven phosphates. Acid phosphatase can hydrolyze three inorganic phosphoanhydrides at higher rates than alkaline phosphatase (Fig. 3a). For example, the hydrolysis rate of P_2 by acid phosphatase (1281.12 ± 129 μM hr^{-1}) is much higher than that by alkaline phosphatase (203.72 ± 15.2 μM hr^{-1}) (Table S1). In contrast, for organic phosphate monoesters, alkaline phosphatase has a higher hydrolysis rate than acid phosphatase (Fig. 3a). For instance, GP as a typical organic phosphate

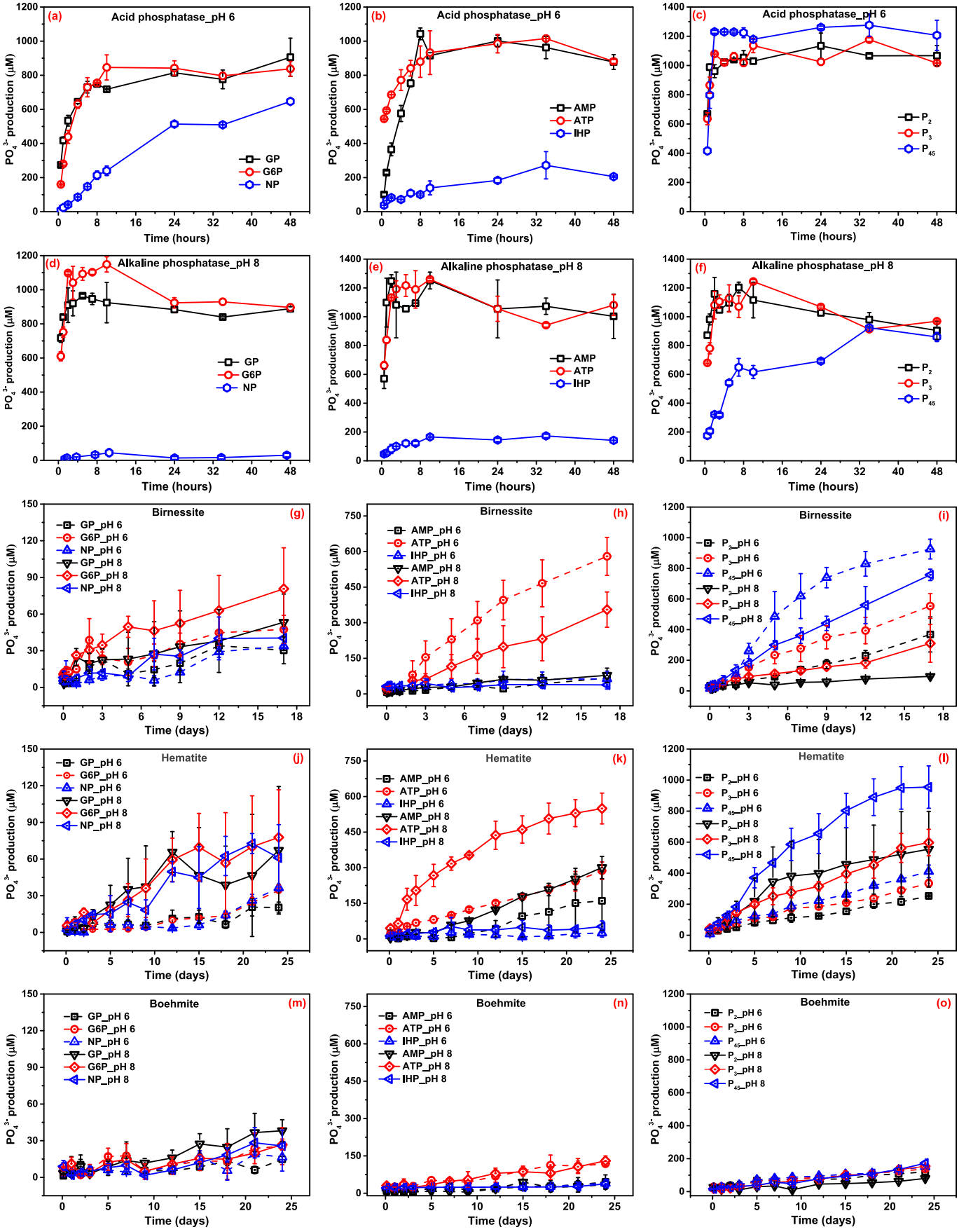

Fig. 2. Dynamics of orthophosphate (PO_4^{3-}) production from enzyme- and mineral-catalyzed hydrolysis of organic phosphates and phosphoanhydrides by acid phosphatase (a-c) at pH 6, alkaline phosphatase (d-f) at pH 8, as well as birnessite (g–i), hematite (j–l), and boehmite (m–o) at pH 6 and 8. Error bars indicate standard deviation (SD) of replicate experiments.

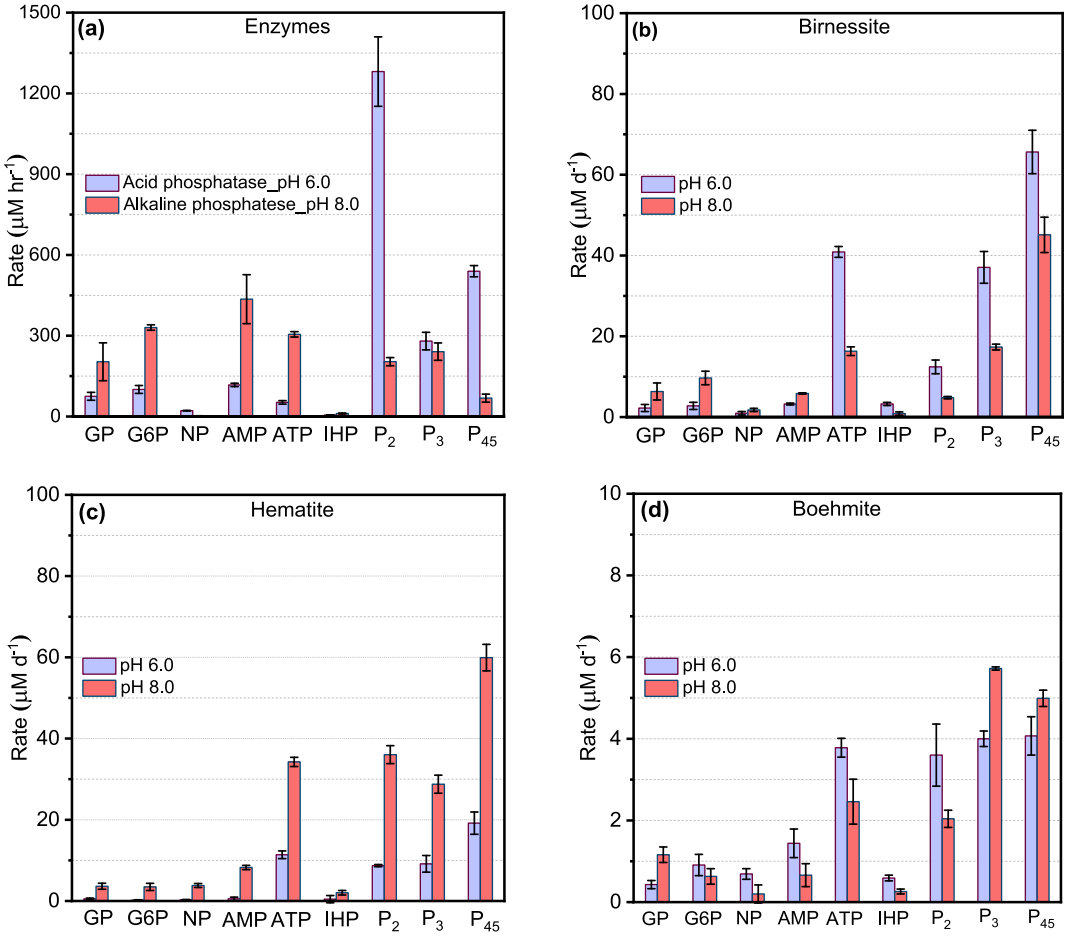

Fig. 3. Fitted rates of the initial linear range for enzyme- and mineral-catalyzed hydrolysis of organic phosphates and inorganic phosphoanhydrides. (a) Hydrolysis rates by acid phosphatase at pH 6 and alkaline phosphatase at pH 8. (b-d) Hydrolysis rates on hematite, birnessite, and boehmite, respectively, at pH 6 and 8. Error bars indicate standard deviation (SD) of replicate experiments. Note the difference in y-axis units.

monoester shows a hydrolysis rate of 75.02 ± 14.8 μM hr^{-1} by acid phosphatase and 203.41 ± 70.4 μM hr^{-1} by alkaline phosphatase (Table S1).

The three minerals have low hydrolysis rates (a few μM d^{-1}) for five organic phosphates, except for ATP which contains both P−O−P (phosphoanhydride) and P−O−C (phosphate ester) bonds (Fig. 3b-d and Table 1). ATP can be viewed as an organic phosphoanhydride (structure in Table 1). The production of orthophosphate from ATP hydrolysis by three minerals may first come from the cleavage of terminal P—O—P bond in the molecule. The hydrolysis rates of three inorganic phosphoanhydrides are an order of magnitude higher than those of phosphate monoesters and are affected by mineral type and solution pH. For the hydrolysis of inorganic phosphoanhydrides, birnessite has a higher rate at pH 6 than 8, while hematite and boehmite have higher rates at pH 8 than pH 6 (Fig. 3b-d). The hydrolysis rates roughly follow the order of birnessite > hematite > boehmite at pH 6, and hematite > birnessite > boehmite at pH 8 (Fig. 3b-d). Regardless of solution pH, birnessite and hematite always display an order of magnitude higher hydrolysis rates (tens of μM d^{-1}) than boehmite (a few μM d^{-1}). Specifically, birnessite, hematite, and boehmite can hydrolyze P_{45} at 65.63, 19.17, and 4.07 μM d^{-1} at pH 6, and 45.12, 59.93, and 4.99 μM d^{-1} at pH 8, respectively (Table S1).

3.3. Preferential hydrolysis of phosphates by enzymes and minerals

Based on the differences in hydrolysis rates of organic phosphates and inorganic phosphoanhydrides, we hypothesize that phosphatases and oxide minerals might have different substrate preferences for phosphate monoesters and phosphoanhydrides. To test this hypothesis, we performed time-resolved solution ^{31}P NMR measurements to investigate the hydrolysis of co-present GP and P_{45} by enzymes or minerals. GP and P_{45} were chosen as a representative organic phosphate monoester and inorganic phosphoanhydride/polyphosphate in natural environments, respectively.

In the presence of acid phosphatase at pH 6, we observed the simultaneous decrease in intensity for the chemical shifts of GP (at 1.68 ppm) and P_{45} middle P groups (at −21.8 ppm), as well as an accompanied increase in the intensity of orthophosphate chemical shift (at 0.44 ppm) (Fig. 4a), suggesting no obvious preference of acid phosphatase in hydrolyzing organic phosphate ester and phosphoanhydride. Due to the higher hydrolysis rate of P_{45} (539.71 ± 20.7 μM hr^{-1}) over GP (75.02 ± 14.8 μM hr^{-1}) by acid phosphatase in the single substrate system (Fig. 3a), the presence of GP probably inhibits the hydrolysis of P_{45} in the binary system to some extent. In contrast, a different trend is observed for alkaline phosphatase (Fig. 4b). During the first 4 h of the hydrolysis, the chemical shift of GP (δ_P = 3.76 ppm) rapidly disappears as the chemical shift of orthophosphate (δ_P = 2.25 ppm) increases to become a dominant P species, while the chemical shift of P_{45} middle P groups (δ_P = −21.66 ppm) shows limited change within this time frame. After the complete disappearance of GP chemical shift (at 8.5 h), P_{45} is gradually hydrolyzed to produce orthophosphate (Fig. 4b). These results indicate that alkaline phosphatase preferentially hydrolyzes organic phosphate monoester in the co-presence of polyphosphate P_{45} (Fig. 4b). This is also consistent with the result that alkaline phosphatase has a higher hydrolysis rate for organic phosphate monoesters than phosphoanhydrides (Fig. 3a).

In the presence of minerals, as the reaction proceeds, the intensity of GP chemical shift shows very limited change, and the chemical shift of

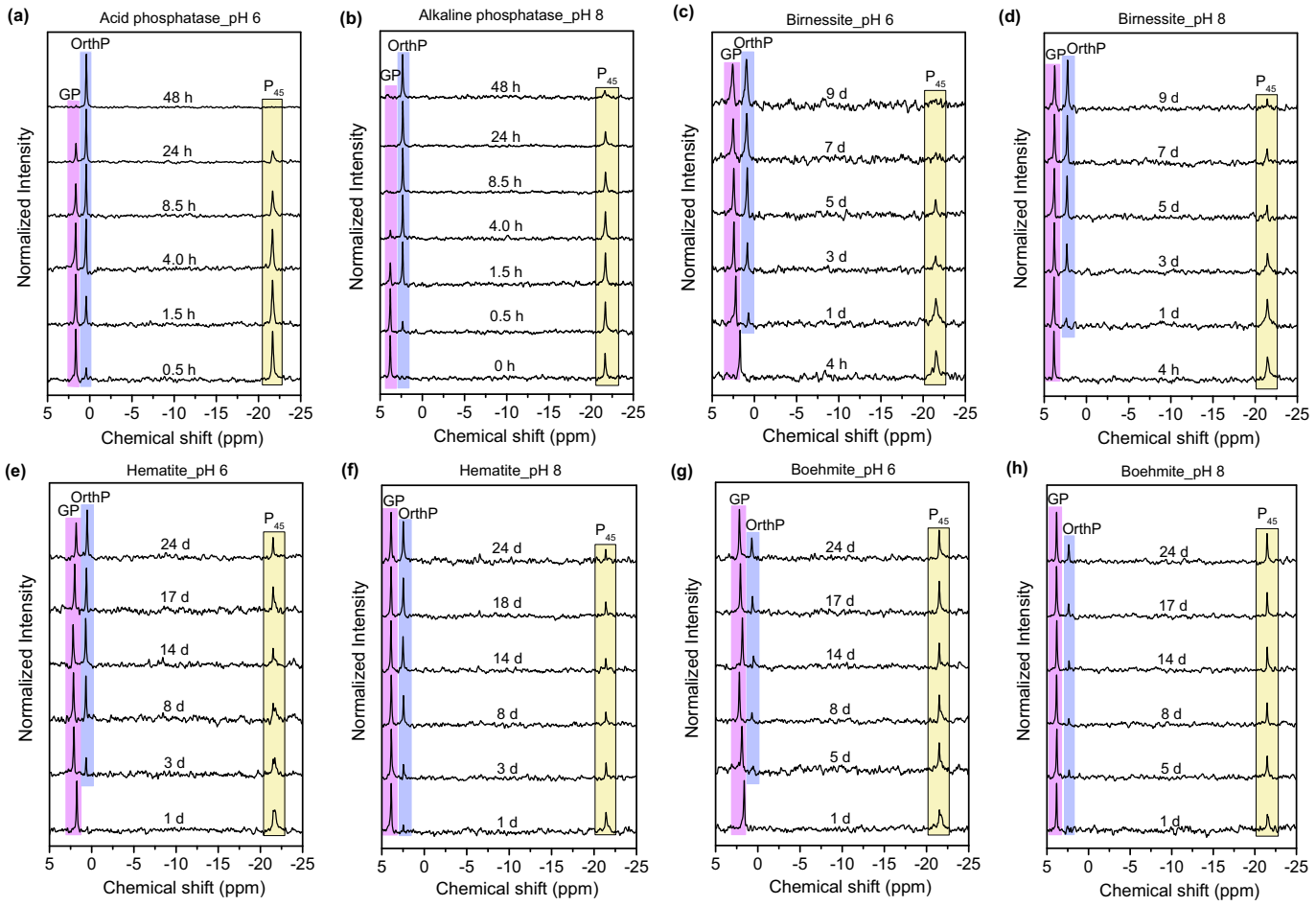

Fig. 4. ^{31}P solution NMR probed P speciation dynamics of glycerophosphate (GP) and polyphosphate (P_{45}) co-hydrolysis by phosphatases and minerals. (a-h) are the time-resolved solution ^{31}P NMR spectra of GP and P_{45} hydrolysis by acid phosphatase at pH 6 (a), alkaline phosphatase at pH 8 (b), as well as birnessite (c, d), hematite (e, f), and boehmite (g, h) at pH 6 and 8, respectively. Purple, blue, and yellow shadings indicate the characteristic chemical shifts of GP, orthophosphate, and polyphosphate's terminal P groups, respectively, and their exact positions are affected by solution pH.

orthophosphate gradually appears and dominates the NMR spectra due to P_{45} hydrolysis (Fig. 3c-h). As shown in the batch experiments (Fig. 2), the three minerals present limited reactivity and have very slow rates toward hydrolyzing organic phosphate monoesters. Although it is difficult to quantify the amount of GP hydrolyzed into orthophosphate using NMR spectroscopy, we hypothesize minimal GP hydrolysis by minerals in the co-presence of P_{45} and that the three minerals prefer to hydrolyze P_{45}, due to the high negative charge of P_{45} and its abundant phosphate groups that can compete to occupy the adsorption sites on the mineral surface. The surface binding of P_{45} may impede the hydrolysis of GP on the surface of oxide minerals. This result is consistent with the observation that hematite, birnessite, and boehmite show higher activity in hydrolyzing phosphoanhydrides than organic phosphate esters (Fig. 3c-d). Overall, these results indicate the different preferences of phosphatases and minerals toward hydrolyzing organic phosphate monoesters and inorganic phosphoanhydrides when these substrates are both present.

3.4. Extrapolation to soil and sediment conditions

With the normalized hydrolysis rate data (Figs. 5-6), we can evaluate the relative contributions of phosphatase and mineral catalyzed processes in different environmental settings, assuming substrate-saturating conditions. We first compiled literature data on the contents and distributions of phosphatases and oxide minerals in soils and sediments (SM *ref 6–31*) (Fig. S2 and Table S3). The estimation calculation of enzyme and mineral contents in soils and sediments could be found in SM *Text S3*. The enzyme contents reported in literature are mainly estimated based on activity measurements and do not represent the actual protein concentration in nature. Our literature review showed that alkaline phosphatase content distributes in a wide range of 0.00005–12.02 unit g^{-1} in sediments and 0.00018–2.27 unit g^{-1} in soils (Fig. S2a and Table S3). Acid phosphatase content is in the range of 0.00004–1.17 unit g^{-1} in soils and sediments. The large range of alkaline phosphatase reactivity in the sediments may be attributed to the abundant microbial activity in aquatic environments (Duhamel et al., 2021; Lidbury et al., 2022). The content distribution of Fe/Al/Mn oxides is around 0.0001–0.7364 g g^{-1} in soils and sediments, and the contents of Fe/Al/Mn oxides in soils are much higher than those in sediments (Fig. S2b and Table S3), probably due to the different origin and diagenesis of these oxide minerals in terrestrial and aquatic environments.

The fitted hydrolysis rates by phosphatases (μM hr^{-1}) or oxide minerals (μM d^{-1}) (Fig. 2 and Table S1) are divided by their studied concentrations to convert the hydrolysis rate units into μmol d^{-1} $unit^{-1}$ phosphatase and μmol d^{-1} g^{-1} mineral (Table S2 and calculation procedures in SM *Text S2*). Then, by multiplying the environmental contents of phosphatases (unit g^{-1}) and minerals (g g^{-1}) in soils and sediments by the initial hydrolysis rates (μmol d^{-1} $unit^{-1}$ for phosphatases or μmol d^{-1} g^{-1} for minerals) for each studied P compound, we obtained the hydrolysis contributions for each phosphate-enzyme/mineral system in soils and sediments with a uniform rate unit of μmol d^{-1} g^{-1}. This normalization allows us to compare the relative significance of organic phosphate ester and phosphoanhydride hydrolysis by phosphatases and minerals in soils and sediments (Figs. 5-6).

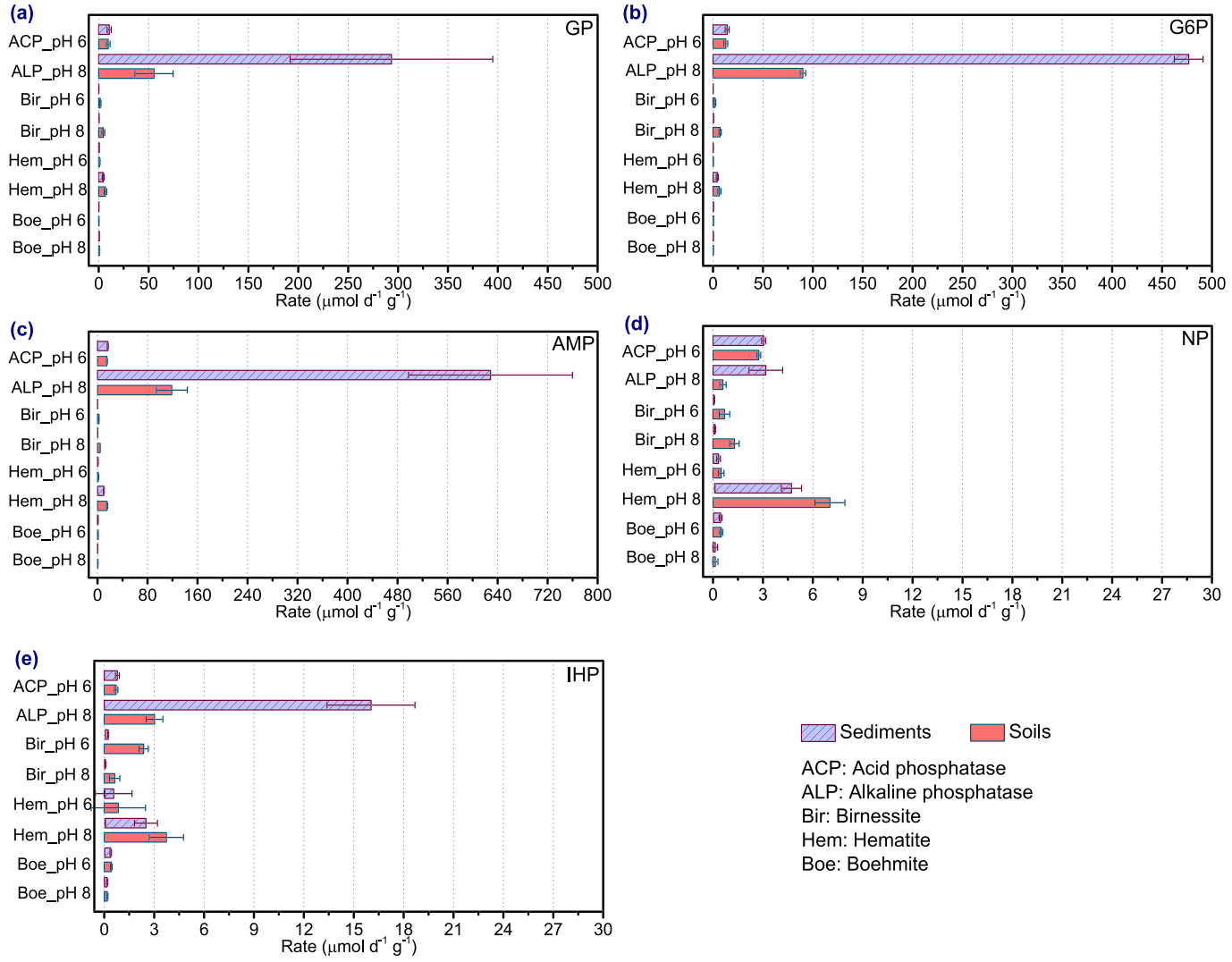

Fig. 5. Estimated range of rates for organic phosphate hydrolysis by acid/alkaline phosphatases and Mn/Fe/Al oxide minerals at pH 6 or 8 in soils and sediments. (a-e) are the estimated data for GP, G6P, AMP, NP, and IHP, respectively. The contents and distribution of these phosphatases and oxide minerals were estimated based on literature data (SM *ref 6–31*) and summarized in SM Fig. S2 and Table S3. Error bars indicate standard deviation (SD) of replicate.

Using this approach, alkaline phosphatase is estimated to significantly contribute to the hydrolysis of organic phosphate monoesters (GP, G6P, and AMP) and the associated hydrolysis rates can reach hundreds of μmol d^{-1} g^{-1} (Fig. 5). Due to the high stability of NP and IHP, their hydrolysis rates by phosphatases and minerals are relatively low at a few μmol d^{-1} g^{-1} regardless of soil or sediment environments (Figs. 5d-e). The hydrolysis rates of the other seven P compounds by acid phosphatase, birnessite, and hematite are similar and estimated to be tens of μmol d^{-1} g^{-1} (Figs. 5-6). Meanwhile, we note that the contribution of alkaline phosphatase to the hydrolysis of three inorganic phosphoanhydrides is similar to or even lower than that of acid phosphatase, birnessite, and hematite (Fig. 6) under some different conditions. Especially for long chain polyphosphate (P_{45}), hematite and birnessite may dominate polyphosphate hydrolysis in soils with hydrolysis rates of 110.3 and 32.9 μmol d^{-1} g^{-1} at pH 8, respectively (Fig. 6d). Regardless of the P species considered, boehmite consistently shows the lowest activity toward hydrolyzing organic phosphates and phosphoanhydrides (Figs. 5-6). Due to the complex matrices of natural environments (e.g., different reactivity of natural minerals vs. lab-synthesized minerals, different solid composition/phases, the presence of organic matters, etc.), this extrapolation is the first and initial attempt on comparing the contribution of abiotic and biotic P remineralization in nature. Future research should warrant to 1) explore a complete evaluation and full comparison between different minerals and enzymes under environmental conditions and 2) reveal the mechanistic roles and reactivities of oxide minerals in the hydrolysis of different P compounds. However, to our knowledge, the current study provides a first direct semi-quantitative comparison of the relative contributions of environmental phosphatases and minerals on P mineralization and gives the initial basis for further exploration on the critical roles of natural minerals in global P cycling.

3.5. Hydrolysis mechanism explanations

The dephosphorylation activity of acid and alkaline phosphatases is attributed to the metal cofactors in the enzyme structure that can form bidentate binding to terminal phosphate groups of the substrate P molecules (Lassila et al., 2011; Yong et al., 2014). For instance, acid phosphatase has an active site containing one Fe(III) and one Mn(II) (Rodriguez et al., 2014), and alkaline phosphatase (PhoA) active site contains two Zn(II) ions (Sunden et al., 2017). Recent studies on the crystal structure of two other alkaline phosphatases (PhoD and PhoX) revealed that the active hydrolysis sites of PhoD contain one Fe(III) and two Ca(II) ions (Rodriguez et al., 2014), whereas PhoX active sites contain two Fe(III) and three Ca (II) ions (Yong et al., 2014). Interestingly, mineral surfaces contain large amounts of surface metal atoms, which that might serve similar functions

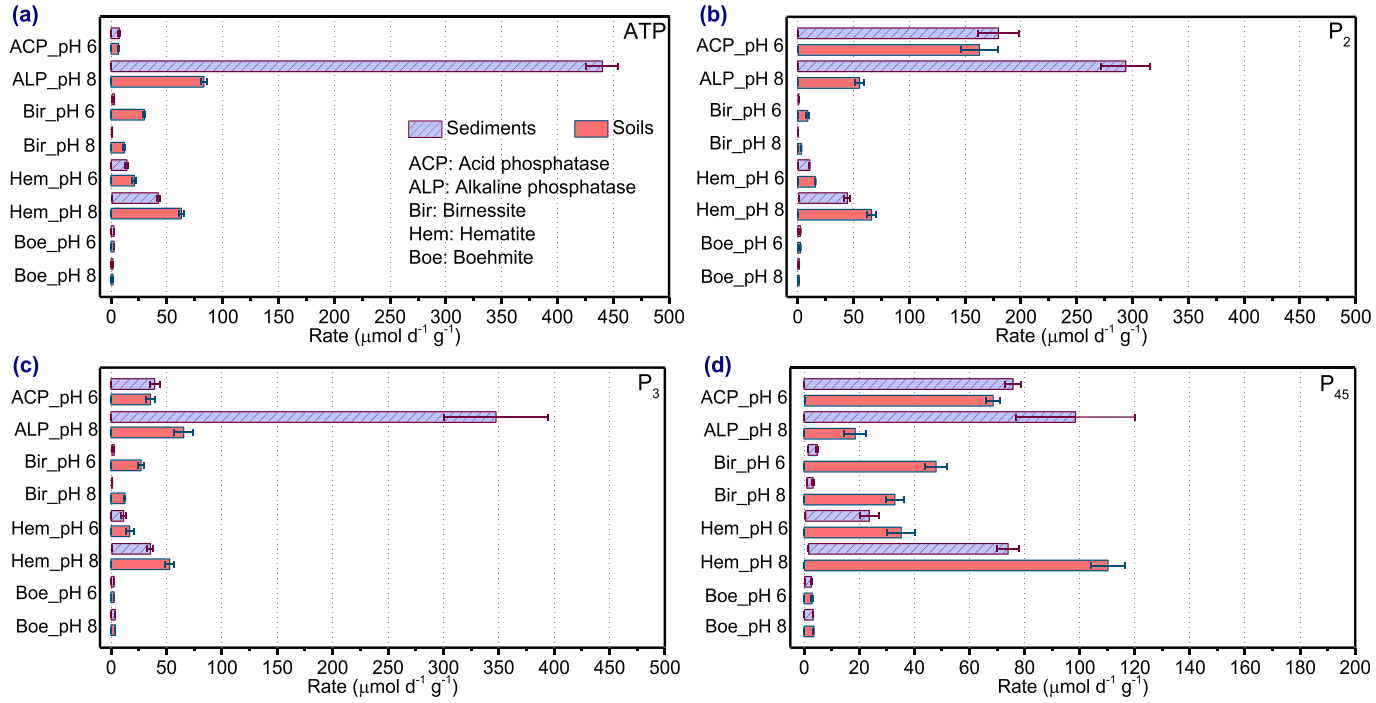

Fig. 6. Estimated range of rates for phosphoanhydride hydrolysis by acid/alkaline phosphatases and Mn/Fe/Al oxide minerals at pH 6 or 8 in soils and sediments. (a-i) are the estimated data for ATP, P_2, P_3, and P_{45}, respectively.

via the formation of inner-sphere complexes with the terminal phosphate groups of the substrate P molecules (Baldwin et al., 2001; Huang, 2018; Wan et al., 2019b). The presumed transition state geometry of bidentate binuclear complexes at the mineral-water interface makes adsorbed phosphate easily attacked by proximally coordinated hydroxyl groups [e.g., μ-(hydr)oxo bridges], leading to the hydrolysis of phosphate esters and phosphoanhydrides (Baldwin et al., 1995; Huang, 2018; Wan et al., 2019b).

For enzymatic dephosphorylation, the biological molecules in the phosphatase structure can promote the dissociation of newly formed orthophosphate from the metal cofactor-phosphate complex (Coleman, 1992), and studies have shown inhibitory effects of orthophosphate on acid and alkaline phosphatase activities (Fernley and Walker, 1967; Srivastava and Anand, 2015). In mineral systems, competitive adsorption onto the mineral surfaces exists between the initial organic phosphate/phosphoanhydride molecules and produced orthophosphate. For long chained polyphosphate (e.g., P_{45}), the produced short chained products can compete for surface adsorption sites to displace the produced orthophosphate and further promote the hydrolysis reaction (Wan et al., 2019b). The weak competitive ability of organic phosphate monoesters suggests that they cannot replace the formed and coordinated orthophosphate. Although IHP has a high negative charge and high adsorption capacity, the coordination geometry of surface IHP complexes may resist nucleophilic attack (Jarosch et al., 2019). We note that the rate of mineral-catalyzed hydrolysis for inorganic phosphoanhydrides is generally positively correlated to the chain length (Fig. 2b-d). The high hydrolysis rate of long chained phosphoanhydrides might be attributed to their higher negative charge and stronger competitive adsorption ability, which promote the dissociation of the produced orthophosphate from the mineral surface and allows continuous proceeding of the hydrolysis reaction (Wan et al., 2019a). The hydrolysis extents and rates of organic phosphates and phosphoanhydrides at the mineral-water interface is also determined by the competitive adsorption and dissociation of newly formed orthophosphate. These results reveal the similarities and differences of enzyme- and mineral-catalyzed pathways for the hydrolysis of organic phosphate esters and phosphoanhydrides (Klein et al., 2019; Olsson et al., 2012; Wan et al., 2019b).

To further explore the effects of extrinsic metal ions on phosphatase and mineral hydrolysis, we conducted hydrolysis experiments of ATP by acid and alkaline phosphatases, hematite, birnessite, and boehmite with or without the presence of 0.5 mM metal cations (Ca^{2+}, Mg^{2+}, Zn^{2+}, and Mn^{2+}) at pH 6 and 8 (Fig. S3). ATP has both phosphoanhydride and phosphate monoester bonds and can be readily hydrolyzed by phosphatases and minerals (Fig. 3). Metal cations have limited impacts on ATP hydrolysis by acid phosphatase at pH 6 but inhibition effects were observed for alkaline phosphatase at pH 8 (Figs. S3a-b), consistent with previous studies (Hoehamer et al., 2005; Huang et al., 2018; Wu et al., 2013). Thus, these extrinsic metal cations cannot directly improve the hydrolysis reactivity of metal co-factors in phosphatase active sites. However, at pH 8, metal cations may strongly complex with the phosphate groups of ATP molecules and inhibit the coupling of ATP terminal phosphate group with the active sites of alkaline phosphatase, subsequently reducing the enzymatic catalysis reaction (Huang et al., 2018). Meanwhile, we observed a promotion effect of metal cations on ATP hydrolysis by hematite and birnessite at different levels, and such effect is more obvious at pH 8 than pH 6 (Figs. S3c-f). This might be explained by the stronger co-sorption and/or complexation of metal cations and phosphate groups on mineral surfaces at pH 8, which increases the chance of hydrolysis reactions for this phosphate molecule (Li et al., 2012; Wan et al., 2019b; Wan et al., 2017). In boehmite suspensions with 0.5 mM metal cations, there was only a slight enhancement in ATP hydrolysis rate, which is likely due to the already low reactivity of boehmite for ATP hydrolysis (Figs. S3g-h). The results of metal cation experiments indicate the different effects of metal cations on ATP hydrolysis by phosphatases and minerals, and such effects are influenced by the types of enzymes, minerals, metal type, and solution pH, which warrant future investigations.

3.6. Discussions on abiotic and biotic P remineralization pathways

Phosphatases and oxide minerals possess different hydrolysis abilities toward organic phosphate esters and phosphoanhydrides (Figs. 1-3) and selective reactivity for different P substrates (Fig. 4). Acid and alkaline phosphatases can hydrolyze phosphate monoesters (except for IHP) and inorganic phosphoanhydrides at high rates (Fig. 2a). The unit contents of the enzymes used in this study is much higher than those in natural environments. By normalizing the hydrolysis rates of phosphatases and oxide

minerals processes to include the environmental activity or contents of these enzymes and minerals, the contribution of mineral-catalyzed phosphoanhydride hydrolysis is estimated to be comparable to enzymatic processes in soils and sediments under some conditions (e.g., high mineral contents) (Fig. 6).

Additionally, in soil environments where pH is usually below 7, alkaline phosphatase activity is potentially lower than our calculated contribution as its activity significantly decreases with the decrease of pHs. Thus mineral-catalyzed hydrolysis as an abiotic process might play significant yet previously overlooked roles in the transformation of phosphoanhydride compounds (e.g., ATP, pyrophosphate, and polyphosphate) in these environments, especially Fe and Mn oxide mineral-enriched soils. Specifically, within three selected oxide minerals, birnessite and hematite show higher hydrolysis activity for phosphoanhydrides (ATP, P_2, P_3, and P_{45}) than organic phosphate esters (Figs. 5-6). Boehmite consistently shows low hydrolysis reactivity for all nine phosphates tested, which may be attributed to its low surface reactivity. The difference in mineral crystal structure might affect the reactivity of oxide minerals toward hydrolyzing different phosphates. Future studies should explore the specific structure of varied phosphate compounds at the mineral-water interface and the influences of crystalline structures and surface properties (e.g., surface area, charge, reactive site type and density) for different Fe, Mn, and Al oxides to provide further mechanistic explanations. Finally, at the mineral-water interface of soils and sediments, abundant oxide minerals might undertake a part of P remineralization as abiotic factors to contribute the P recycle and reuse since a large amount of organic P are easily associated with natural oxide minerals (Baldwin, 2013; Ruttenberg and Sulak, 2011; Zhu et al., 2018). Since Fe and Mn oxides are sensitive to redox fluctuations, these minerals could be reduced to aqueous Fe^{2+} and Mn^{2+} in anoxic environments (e.g., the reducing layers of soils or sediments) (Scholtysik et al., 2022), leading to the low contribution of mineral-catalyzed P remineralization. Thus, it is likely that abiotic P remineralization undertaken by natural oxide minerals can occur in the oxic layers of soils and sediments and alkaline phosphatase might significantly undertake biotic remineralization of organic phosphates and phosphoanhydrides in aquatic environments.

The current study has used a simplified treatment to reveal the important contributions of natural oxide minerals to the degradation and remineralization of organic phosphates and phosphoanhydrides in soil and sediment environments. The further efforts and new research tools should be applied to track and distinguish abiotic and biotic P mineralization pathways. For example, phosphate oxygen isotope has been used to understand the interplay of biotic and abiotic processes on P cycling in natural environments. Phosphate oxygen isotope exchange in a mineral-water-biota system (including mineral surface, aqueous phase, and bacterial cells) was modelled to indicate that the rate of biological uptake of P was the major factor controlling the changes of phosphate isotope composition (Jaisi et al., 2017). Additionally, using isotopic dilution approaches, a previous study indicated that typical basal gross organic P remineralization rates range between 0.003 and 0.08 μmol P d^{-1} g^{-1} in arable soils, but the rates can be up to 0.4 μmol P d^{-1} g^{-1} in grassland and forest soils (Bünemann, 2015). The author also pointed out that soil organic P remineralization rates determined by phosphomonoesterase activity measurements are one to two orders of magnitude greater than those determined by isotopic dilution. Our calculated values based on laboratory-controlled experiments are slightly larger than those observed in soils and sediments, likely due to the difference in analytical methods, as well as the potential influences of complex environmental matrices with various physiochemical conditions (e.g., pH variation, different redox potential, different solid composition, different abundance of varied P compounds, presence of organic and inorganic substances) (Wang et al., 2019; Wang et al., 2020; Zhu et al., 2018). The alkaline phosphatase-harboring bacterial community associated with arbuscular mycorrhizal hyphae was reported to be significantly changed in response to different P sources, with *Pseudomonas* being higher relative abundance in organic P treatments than inorganic P ones (Wang et al., 2019).

Finally, our study provides a first semi-quantitative comparison of the relative contributions of biotic and abiotic processes for the transformation and remineralization of organic phosphate and phosphoanhydride molecules. Our results broaden the current state of knowledge on the roles of enzymes and minerals in P transformation, remineralization, and cycling via biotic and abiotic controls in natural systems. Future research is warranted to provide mechanistic explanations for surface-catalyzed phosphate hydrolysis at the molecular level and to further explore the critical roles of natural minerals in P remineralization and cycling in the environments.

3.7. Environmental implications

In the global P cycle, it is commonly accepted that microbes/plants undertake a biological role by regulating the *degradation* (e.g., hydrolysis) of complex P compounds and *production* of orthophosphate (e.g., remineralization), whereas natural minerals play geochemical roles in controlling the *sequestration* and *immobilization* (e.g., adsorption, desorption, precipitation, and dissolution) of environmental phosphates (Defforey and Paytan, 2018). The current research is a first simplified evaluation toward understanding the potential overlooked roles of natural oxide minerals as an inorganic *catalyst* in global P cycling. This study implies that natural minerals can play significant roles in catalyzing the *degradation* and *hydrolysis* of complex P compounds and *production* of orthophosphate, not just presents as a P *sink* or *source* to fix P on the surface. This finding highlights a previously overlooked pathway for environmental P remineralization and provides new insights for understanding the global P cycle. For instance, in the surficial layers of lake and marine sediments where the rapid transformation of phosphoanhydrides (e.g., polyphosphate) into orthophosphate occurs during the diagenesis, both enzyme- and mineral-catalyzed hydrolysis may play an important role in regulating the remineralization and transformation of phosphoanhydrides or other phosphate species at the sediment-water interface (Diaz et al., 2008; Hupfer et al., 2004). Such roles of natural minerals were not previously appreciated, and our study presents a shift in paradigm for constraining P biogeochemical cycling by revisiting the roles of minerals as abiotic catalysts in addition to their traditionally accepted roles as geological P sequestration.

4. Conclusions

Our study indicates that both enzymes and minerals can hydrolyze organic phosphate esters and phosphoanhydrides to various extents and have different substrate preferences. Alkaline phosphatase hydrolyzes phosphate monoesters at a faster rate than phosphoanhydrides, whereas acid phosphatase and minerals show faster rates toward inorganic phosphoanhydrides than phosphate monoesters. After the normalization to the natural reactivity/abundance of enzymes and minerals, abiotic (mineral-catalyzed) P remineralization rates of phosphoanhydrides are comparable to biotic one mediated by phosphatases. Thus, mineral-catalyzed P hydrolysis might play a critical but previously overlooked role in environmental P cycle as they contribute to the remineralization of complex P molecules in addition to the traditionally viewed role as a P sequestration sink.

CRediT authorship contribution statement

B.W. and Y.T. conceived the research idea and designed the experiments. B.W. conducted experiments, analyzed the data, and wrote the manuscript. Y.T. supervised the study. R.H. and J.D provided guidance during the experiments. All authors discussed the results and edited the manuscript.

Declaration of competing interest

The authors declare that they have no known competing financial interests or personal relationships that could have appeared to influence the work reported in this paper.

Acknowledgements

This work is supported by NASA Grant# 80NSSC21K0483 and NSF Grants# 1559087, 1739884, and 2108688. JMD acknowledges support from NSF Grants # 1559124 and 2015310.

Appendix A. Supplementary data

Supplementary data to this article can be found online at https://doi.org/10.1016/j.scitotenv.2022.155187.

References

Baldwin, D.S., 2013. Organic phosphorus in the aquatic environment. Environ. Chem. 10, 439–454.
Baldwin, D.S., Beattie, J.K., Coleman, L.M., Jones, D.R., 1995. Phosphate ester hydrolysis facilitated by mineral phases. Environ. Sci. Technol. 29, 1706–1709.
Baldwin, D.S., Beattie, J.K., Coleman, L.M., Jones, D.R., 2001. Hydrolysis of an organophosphate ester by manganese dioxide. Environ. Sci. Technol. 35, 713–716.
Bünemann, E.K., 2015. Assessment of gross and net mineralization rates of soil organic phosphorus – a review. Soil Biol. Biochem. 89, 82–98.
Canfield, D.E., Erik, K., Bo, T., 2005. The phosphorus cycle. In: Canfield, D.E., Kristensen, E., Thamdrup, B. (Eds.), Advances in Marine Biology. Academic Press, pp. 419–440.
Chen, M., Ding, S., Chen, X., Sun, Q., Fan, X., Lin, J., Ren, M., Yang, L., Zhang, C., 2018. Mechanisms driving phosphorus release during algal blooms based on hourly changes in iron and phosphorus concentrations in sediments. Water Res. 133, 153–164.
Coleman, J.E., 1992. Structure and mechanism of alkaline phosphatase. Annu. Rev. Biophys. Biomol. Struct. 21, 441–483.
Defforey, D., Paytan, A., 2018. Phosphorus cycling in marine sediments: advances and challenges. Chem. Geol. 477, 1–11.
Diaz, J., Ingall, E., Benitez-Nelson, C., Paterson, D., de Jonge, M.D., McNulty, I., Brandes, J.A., 2008. Marine polyphosphate: a key player in geologic phosphorus sequestration. Science 320, 652–655.
Duhamel, S., Diaz, J.M., Adams, J.C., Djaoudi, K., Steck, V., Waggoner, E.M., 2021. Phosphorus as an integral component of global marine biogeochemistry. Nat. Geosci. 14, 359–368.
Fernley, H.N., Walker, P.G., 1967. Studies on alkaline phosphatase. Inhibition by phosphate derivatives and the substrate specificity. Biochem. J. 104, 1011–1018.
Figueroa, I.A., Coates, J.D., 2017. Microbial phosphite oxidation and its potential role in the global phosphorus and carbon cycles. In: Sariaslani, S., Gadd, G.M. (Eds.), Advances in Applied Microbiology. Academic Press, pp. 93–117.
Golotin, V., Balabanova, L., Likhatskaya, G., Rasskazov, V., 2015. Recombinant production and characterization of a highly active alkaline phosphatase from marine bacterium cobetia marina. Mar. Biotechnol. 17, 130–143.
Hoehamer, C.F., Mazur, C.S., Wolfe, N.L., 2005. Purification and partial characterization of an acid phosphatase from spirodelaoligorrhiza and its affinity for selected organophosphate pesticides. J. Agric. Food Chem. 53, 90–97.
Huang, X.L., 2018. Hydrolysis of phosphate esters catalyzed by inorganic iron oxide nanoparticles acting as biocatalysts. Astrobiology 18, 294–310.
Huang, R., Wan, B., Hultz, M., Diaz, J.M., Tang, Y., 2018. Phosphatase-mediated hydrolysis of linear polyphosphates. Environ. Sci. Technol. 52, 1183–1190.
Hupfer, M., Ruübe, B., Schmieder, P., 2004. Origin and diagenesis of polyphosphate in lake sediments: a 31P-NMR study. Limnol. Oceanogr. 49, 1–10.
Jaisi, D.P., Hou, Y., Stout, L.M., Massoudieh, A., 2017. Modeling of biotic and abiotic processes affecting phosphate oxygen isotope ratios in a mineral-water-biota system. Water Res. 126, 262–273.
Jarosch, K.A., Kandeler, E., Frossard, E., Bünemann, E.K., 2019. Is the enzymatic hydrolysis of soil organic phosphorus compounds limited by enzyme or substrate availability? Soil Biol. Biochem. 139, 107628.
Karl, D.M., 2014. Microbially mediated transformations of phosphorus in the sea: new views of an old cycle. Annu. Rev. Mar. Sci. 6, 279–337.
Klein, A.R., Bone, S.E., Bakker, E., Chang, Z., Aristilde, L., 2019. Abiotic phosphorus recycling from adsorbed ribonucleotides on a ferrihydrite-type mineral: probing solution and surface species. J. Colloid Interf. Sci. 547, 171–182.
Lassila, J.K., Zalatan, J.G., Herschlag, D., 2011. Biological phosphoryl-transfer reactions: understanding mechanism and catalysis. Annu. Rev. Biochem. 80, 669–702.
Li, W., Xu, W., Parise, J.B., Phillips, B.L., 2012. Formation of hydroxylapatite from co-sorption of phosphate and calcium by boehmite. Geochim. Cosmochim. Acta 85, 289–301.
Lidbury, I.D.E.A., Scanlan, D.J., Murphy, A.R.J., Christie-Oleza, J.A., Aguilo-Ferretjans, M.M., Hitchcock, A., Daniell, T., 2022. A widely distributed phosphate-insensitive phosphatase presents a route for rapid organophosphorus remineralization in the biosphere. Proc. Natl. Acad. Sci. U. S. A. 119, e2118122119. https://doi.org/10.1073/pnas.2118122119.
Liu, J., Cade-Menun, B.J., Yang, J., Hu, Y., Liu, C.W., Tremblay, J., LaForge, K., Schellenberg, M., Hamel, C., Bainard, L.D., 2018. Long-term land use affects phosphorus speciation and the composition of phosphorus cycling genes in agricultural soils. Front. Microbiol. 9, 1643.
Murphy, J., Riley, J.P., 1962. A modified single solution method for the determination of phosphate in natural waters. Anal. Chim. Acta 27, 31–36.
Olsson, R., Giesler, R., Loring, J.S., Persson, P., 2012. Enzymatic hydrolysis of organic phosphates adsorbed on mineral surfaces. Environ. Sci. Technol. 46, 285–291.
Paytan, A., McLaughlin, K., 2007. The oceanic phosphorus cycle. Chem. Rev. 107, 563–576.
Recena, R., Cade-Menun, B.J., Delgado, A., 2018. Organic phosphorus forms in agricultural soils under Mediterranean climate. Soil Sci. Soc. Am. J. 82, 783–795.
Rodriguez, F., Lillington, J., Johnson, S., Timmel, C.R., Lea, S.M., Berks, B.C., 2014. Crystal structure of the Bacillus subtilis phosphodiesterase PhoD reveals an iron and calcium-containing active site. J. Biol. Chem. 289, 30889–30899.
Ruttenberg, K.C., 2014. The global phosphorus cycle. In: Turekian, K.K. (Ed.), Treatise on Geochemistry, Second edition Elsevier, Oxford, pp. 499–558.
Ruttenberg, K.C., Sulak, D.J., 2011. Sorption and desorption of dissolved organic phosphorus onto iron (oxyhydr)oxides in seawater. Geochim. Cosmochim. Acta 75, 4095–4112.
Scholtysik, G., Goldhammer, T., Arz, H.W., Moros, M., Littke, R., Hupfer, M., 2022. Geochemical focusing and burial of sedimentary iron, manganese, and phosphorus during lake eutrophication. Limnol. Oceanogr. https://doi.org/10.1002/lno.12019.
Srivastava, P.K., Anand, A., 2015. The inhibitory effect of metals and other ions on acid phosphatase activity from Vigna aconitifolia seeds. Prep. Biochem. Biotechnol. 45, 33–41.
Sunden, F., AlSadhan, I., Lyubimov, A., Doukov, T., Swan, J., Herschlag, D., 2017. Differential catalytic promiscuity of the alkaline phosphatase superfamily bimetallo core reveals mechanistic features underlying enzyme evolution. J. Biol. Chem. 292, 20960–20974.
Thingstad, T.F., Krom, M.D., Mantoura, R.F.C., Flaten, G.A.F., Groom, S., Herut, B., Kress, N., Law, C.S., Pasternak, A., Pitta, P., Psarra, S., Rassoulzadegan, F., Tanaka, T., Tselepides, A., Wassmann, P., Woodward, E.M.S., Riser, C.W., Zodiatis, G., Zohary, T., 2005. Nature of phosphorus limitation in the ultraoligotrophic eastern Mediterranean. Science 309, 1068–1071.
Van Mooy, B.A.S., Krupke, A., Dyhrman, S.T., Fredricks, H.F., Frischkorn, K.R., Ossolinski, J.E., Repeta, D.J., Rouco, M., Seewald, J.D., Sylva, S.P., 2015. Major role of planktonic phosphate reduction in the marine phosphorus redox cycle. Science 348, 783–785.
Wan, B., Yan, Y.P., Zhu, M.Q., Wang, X.M., Liu, F., Tan, W.F., Feng, X.H., 2017. Quantitative and spectroscopic investigations of the co-sorption of myo-inositol hexakisphosphate and cadmium(II) on to haematite. Eur. J. Soil Sci. 68, 374–383.
Wan, B., Huang, R., Diaz, J.M., Tang, Y., 2019a. Manganese oxide catalyzed hydrolysis of polyphosphates. ACS Earth Space Chem. 3, 2623–2634.
Wan, B., Huang, R., Diaz, J.M., Tang, Y., 2019b. Polyphosphate adsorption and hydrolysis on aluminum oxides. Environ. Sci. Technol. 53, 9542–9552.
Wan, B., Yang, P., Jung, H., Zhu, M., Diaz, J.M., Tang, Y., 2021. Iron oxides catalyze the hydrolysis of polyphosphate and precipitation of calcium phosphate minerals. Geochim. Cosmochim. Acta 305, 49–65.
Wang, X., Zhu, M., Koopal, L.K., Li, W., Xu, W., Liu, F., Zhang, J., Liu, Q., Feng, X., Sparks, D.L., 2016. Effects of crystallite size on the structure and magnetism of ferrihydrite. Environ. Sci. Nano 3, 190–202.
Wang, F., Kertesz, M.A., Feng, G., 2019. Phosphorus forms affect the hyphosphere bacterial community involved in soil organic phosphorus turnover. Mycorrhiza 29, 351–362.
Wang, Q., Zhang, C., Liu, P., Jung, H., Wan, B., Patel, D., Pavlostathis, S., Tang, Y., 2020. Effect of interstage hydrothermal treatment on anaerobic digestion of sewage sludge: speciation evolution of phosphorus, iron, and sulfur. ACS Sustain. Chem. Eng. 8, 16515–16525.
Wood, T.I.M., Bormann, F.H., Voigt, G.K., 1984. Phosphorus cycling in a northern hardwood Forest: biological and chemical control. Science 223, 391–393.
Wu, H., Li, D., Zhu, B., Cheng, J., Sun, J., Wang, F., Yang, Y., Song, Y., Yu, C., 2013. Purification and characterization of alkaline phosphatase from the gut of sea cucumber Stichopus japonicus. Fish. Sci. 79, 477–485.
Yan, Y., Li, W., Yang, J., Zheng, A., Liu, F., Feng, X., Sparks, D.L., 2014. Mechanism of myo-inositol hexakisphosphate sorption on amorphous aluminum hydroxide: spectroscopic evidence for rapid surface precipitation. Environ. Sci. Technol. 48, 6735–6742.
Yong, S.C., Roversi, P., Lillington, J., Rodriguez, F., Krehenbrink, M., Zeldin, O.B., Garman, E.F., Lea, S.M., Berks, B.C., 2014. A complex iron-calcium cofactor catalyzing phosphotransfer chemistry. Science 345, 1170–1173.
Zhu, Y., Feng, W., Liu, S., He, Z., Zhao, X., Liu, Y., Guo, J., Giesy, J., Wu, F., 2018. Bioavailability and preservation of organic phosphorus in lake sediments: insights from enzymatic hydrolysis and 31P nuclear magnetic resonance. Chemosphere 211, 50–61.